12-1994

Optical-fiber Preamplifiers for Ladar Detection and Associated Measurements for Improving the Signal-to-noise Ratio

Michael S. Salisbury
Technology Scientific Services Inc.

Paul F. McManamon
U.S. Air Force

Bradley D. Duncan
University of Dayton, bduncan1@udayton.edu

Optical-fiber preamplifiers for ladar detection and associated measurements for improving the signal-to-noise ratio

Michael S. Salisbury
Technology Scientific Services Inc.
P.O. Box 3065
Overlook Branch
Dayton, Ohio 45431

Paul F. McManamon, MEMBER SPIE
Wright Laboratory AARI-2
Electro-Optic Sensors
Wright Patterson Air Force Base, Ohio
45433-6543

Bradley D. Duncan, MEMBER SPIE
University of Dayton
Center for Electro-Optics
300 College Park
Dayton, Ohio 45469-0226

Abstract. In an effort to increase achievable postdetection signal-to-noise ratios (SNRs) of continuous-wave, 1-μm all-solid-state ladar systems, a prototype rare-earth-doped optical-fiber amplifier has been included in the optical return signal path of both a heterodyne and a direct-detection ladar system. We provide numerical predictions for SNR increases according to our previously developed theory. We also detail our experimental efforts and provide the results of SNR measurements for four distinct cases: direct ladar detection with and without a fiber amplifier, and heterodyne ladar detection with and without a fiber amplifier. Experimentally measured increases in SNRs for ladar systems incorporating an optical-fiber amplifier are then compared with our earlier predictions. Specifically, we have found that for direct detection with a fiber amplifier in place, the predicted SNR increase is 42.0 dB, and we have measured an increase of 36.5 dB. Similarly, for heterodyne ladar detection with a fiber amplifier, the predicted SNR increase is 3.8 dB, and we have measured an increase of 8.0 dB.

Subject terms: ladar, laser radar; fiber amplifier; signal-to-noise ratio.

Optical Engineering 33(12), 4023–4032 (December 1994).

1 Introduction

In remote sensing, the detection of weak return signals is of vital importance. One method of increasing the sensitivity of an optical remote-sensing device, such as a ladar system, is to optically amplify the return signal before detection. As we have previously shown,[1,2] rare-earth-doped optical-fiber amplifiers offer a compact and lightweight means of optical preamplification appropriate for integration into a ladar system.

In our previous analysis, we developed signal-to-noise ratio (SNR) relationships for direct and heterodyne detection ladar systems, both with and without an optical-fiber amplifier included. We then chose a practical minimum "threshold" SNR of 6 dB as being necessary for reliable target detection. Based then on predicted environmental and electronic noise factors, we determined the signal power required for each ladar detection scheme such that the threshold SNR was achieved. After defining the increase in optical sensitivity to be the difference (expressed in dB) in optical signal powers necessary to achieve the threshold electrical SNR for corresponding ladar systems with and without an optical-fiber amplifier, the sensitivity increases achievable by incorporating an optical-fiber amplifier were determined for both heterodyne and direct-detection ladar schemes. Specifically, our results indicated optical sensitivity increases of 20.6 and 0.73 dB for the direct and heterodyne ladar detection cases, respectively, where we note that the lower sensitivity increase for the heterodyne detection case is due primarily to the already near-optimum performance of an unamplified heterodyne detection scheme, assumed to be adjusted for local-oscillator shot-noise-limited detection.[1,2] In this paper we take the electrical SNR equations used in the previous sensitivity calculations, add efficiency terms encountered in the experimental incorporation of the fiber amplifier, and calculate theoretical electrical SNR increases. We were required to make these measurements by our inability to measure directly the small optical return signal power, as will be seen later in Sec. 3.

This paper discusses the experimental procedures used to verify the equations derived in our previous analysis. For our experimental work, a SNR measurement was first taken for both direct and heterodyne detection without a fiber amplifier. With the same return signal power, corresponding SNR measurements were then taken with a fiber amplifier included. These results were then compared to give the increase in SNR due to the inclusion of the fiber amplifier.

In Sec. 2 of this paper we describe the experimental ladar system, specifically accounting for efficiency terms encountered while incorporating the fiber amplifier, and then examine various issues involved in data collection. In Sec. 3 we use our previous work to predict SNR increases for both

Paper 26024 received Feb. 14, 1994; revised manuscript received Jun. 25, 1994; accepted for publication Jun. 26, 1994.

direct and heterodyne ladar detection with a fiber amplifier included. We present our experimental data and compare them with our theoretical predictions in Sec. 4; in Sec. 5 we summarize our work and examine future research possibilities.

2 Ladar System Overview

In this section we provide an overview of the ladar system, focusing on some aspects of the design that have affected our experimental work. The ladar system with the fiber amplifier inserted is shown for direct and heterodyne detection in Figs. 1 and 2, respectively. As shown in Fig. 1, for direct detection a Nd:YAG laser provides 40 mW of linearly polarized output at a wavelength of 1.064 μm. The laser output then passes through a Faraday optical isolator to prevent backscatter from other optical components in the system from reentering the laser head. The beam then passes through a *variable-ratio attenuator* consisting of a half-wave plate in a rotatable stage and a polarizing beamsplitter cube. As will be discussed in detail later, this is used to reduce the transmitted optical power to levels appropriate for the targets we have used. Also note that as the photodetector we chose to use is ac coupled, the beam is modulated by an optical chopper operating at 2 kHz.

After passing through the variable-ratio attenuator, the beam passes through a *transmit-receive* (TR) *switch*, consisting of a polarizing beamsplitter cube and a Faraday optical rotator used to rotate the outgoing beam polarization by 45 deg. The beam then travels to the target, after which the backscattered optical return signal received from the target is rotated an additional 45 deg by the optical rotator. The polarization of the received signal light is thus perpendicular to the original outgoing light and is reflected by the polarizing beamsplitter cube into the return signal leg.

The return signal from the target then passes through a dichroic mirror and is coupled into the core of a Rutgers University Nd^{+3}-doped optical fiber,[3] whose double cladding configuration is shown in Fig. 3, while pump light from an 850-nm laser diode is simultaneously reflected off the dichroic mirror and coupled into the rectangular inner cladding of the doped fiber.[4] As the pump light travels through the fiber, it passes through the core and creates a population inversion in the rare-earth dopant, and the return signal is then amplified as it passes through the core. Note that due to typically small return signals, the fiber amplifier is operated in the small-signal regime. Thus, spontaneous emission from the upper lasing level is simply added to the amplified return signal. We will see the effects of this spontaneous emission power later.

To couple the amplified return signal out of the fiber amplifier, there is a single-mode AT&T ST-type connector at the end of the fiber amplifier. The double cladding geometry of the doped fiber, however, resulted in severe misalignment of the single-mode core within the ST connector, which was designed for standard circular 125-μm-diam fibers. The buffer on the Rutgers fiber is made of a hard polymer, while the 125-μm outer cladding of the fiber, which would fit into the connector snugly, is made of a soft polymer (see Fig. 3). Several attempts were made to remove the buffer without stripping off the outer cladding, but all were unsuccessful. With the buffer and outer cladding removed, only the rectangular inner cladding and core are left for insertion into the connector, making it very difficult to align the core at the center of the connector. Thus, in order to couple the light out of the fiber amplifier and into another, nondoped single-mode fiber, the ST connector on the nondoped fiber was placed in a fixed mount. The connector on the end of the fiber amplifier was then fixed to a three-axis positioner, and index-matching gel was used to provide good coupling between the fibers as the positioner was used to align the two cores manually. The resulting coupling ratios were consistently about 75%, allowing enough throughput power for experimental data to be taken. This will be included in the optical-efficiency in the equations of the next section.

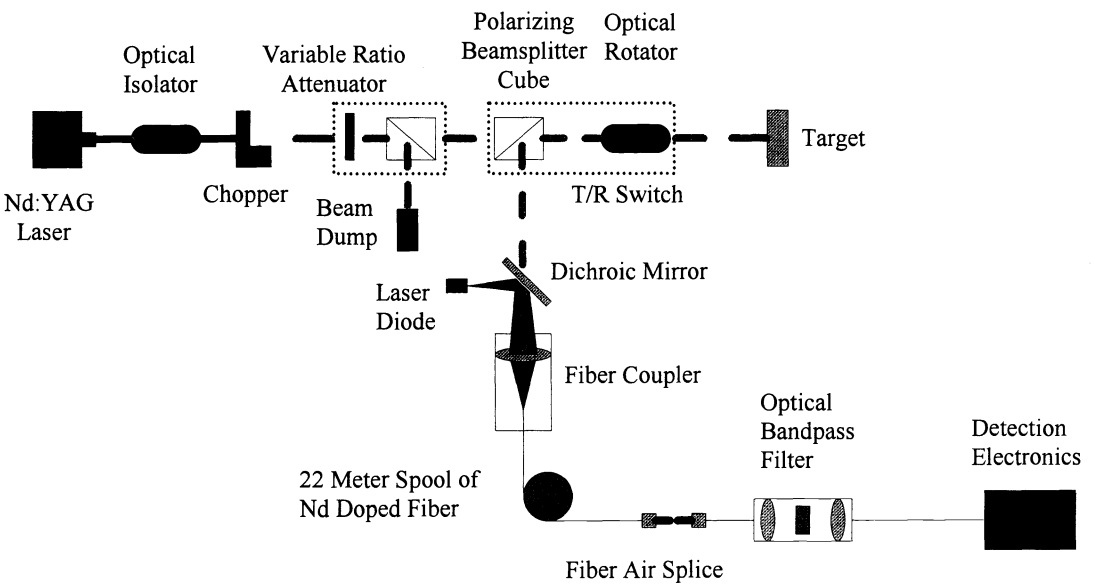

Fig. 1 Direct-detection ladar system. This figure shows the 1.064-μm ladar in its direct-detection configuration. The variable-ratio attenuator and TR switch are outlined, and the fiber amplifier is shown inserted into the return signal leg.

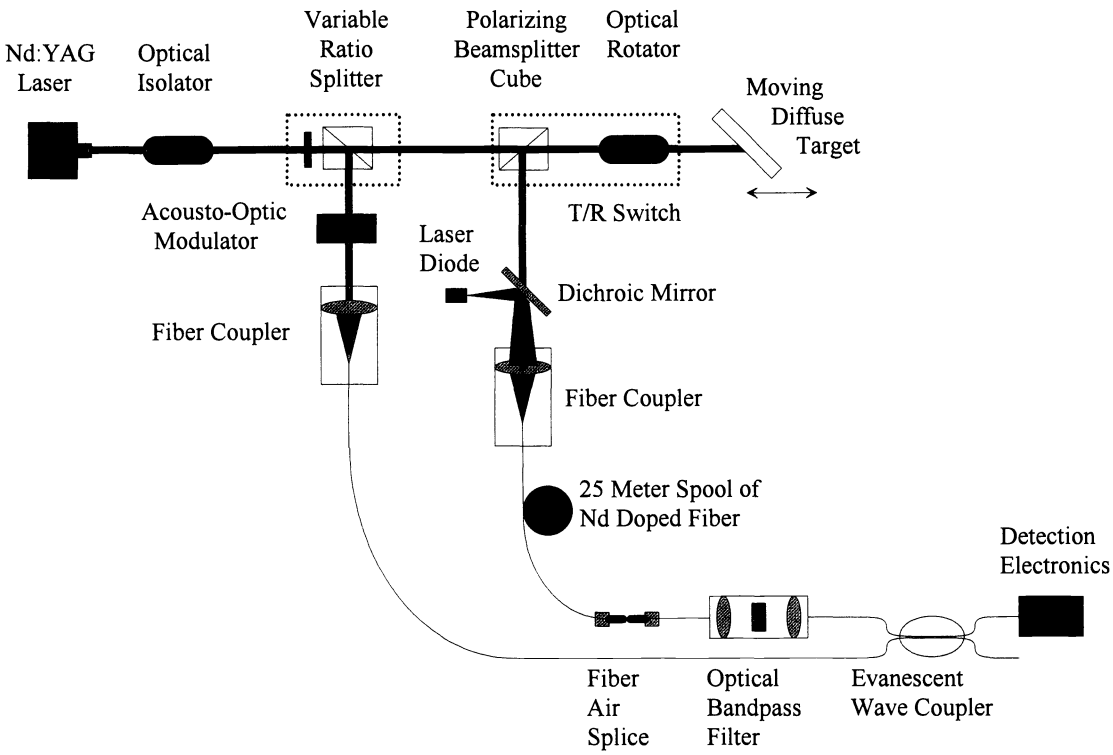

Fig. 2 Heterodyne-detection ladar system. This figure shows the 1.064-μm ladar in its heterodyne-detection configuration. The variable-ratio splitter and TR switch are outlined, and the fiber amplifier is shown inserted into the return signal leg.

The power coupled out of the fiber amplifier at this point includes the amplified return signal, broadband spontaneous-emission power, and any unabsorbed pump power. A 4-nm optical bandpass filter, centered at 1.064 μm, is thus used to eliminate the excess pump light (at 850 nm), as well as any spontaneous-emission power outside of the 1.064 ± 0.002-μm wavelength range. The 75% transmissivity of the optical filter's passband will also be allowed for in the optical-efficiency factors of the next section. After the optical filter, the light is coupled into a multimode fiber pigtailed to the InGaAs PIN detector package, from which the output is amplified and measured with a spectrum analyzer. For clarity, the amplification and detection electronics are schematically shown in Fig. 4, where we note that for direct detection g is the voltage gain of an Analog Modules electronic amplifier and R_{amp} is its input impedance (see Table 1).

For the heterodyne detection scheme shown in Fig. 2, the laser provides both the local-oscillator (LO) power and the power for the transmitted signal. A half-wave plate and polarizing beamsplitter cube are thus used as a *variable-ratio splitter* to vary the amount of power split into the local oscillator leg. The LO is then frequency shifted 200 MHz by an acousto-optic modulator (AOM), and the unshifted zero-order beam out of the AOM is blocked with a beam dump to minimize stray reflections in the system. The frequency-shifted first order is then coupled into a single-mode fiber leading to an evanescent wave coupler, which couples 10% of the LO power into the output fiber leading to the photodetection circuitry. The resulting LO level is set to approach the manufacturer's specified detector saturation level of 200 μW.

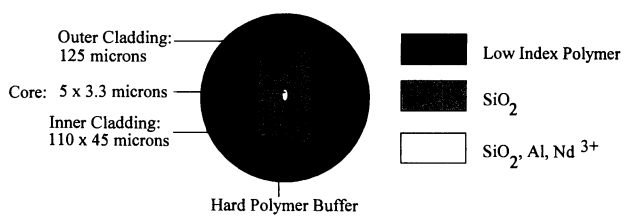

Fig. 3 Geometry of the Rutgers neodymium-doped fiber. The geometry of the Rutgers fiber is shown here. The unusual aspect of the fiber is the rectangular inner cladding used to couple the pump light from the laser diode into the fiber.

Laser power not split into the LO path passes through the TR switch and is reflected off the target. The somewhat depolarized return[5] from the target passes through the TR switch again, which directs a linearly polarized portion into the signal leg. The light reflected into the signal leg passes through a dichroic mirror and is coupled into the fiber amplifier along with the pump light from the laser diode, as discussed previously. The air splice is once again used to couple the power from the fiber amplifier into the nondoped single-mode fiber leading to the free-space fiber-to-fiber coupler, where the 4-nm bandpass filter is inserted into the beam path. These two losses are the same as occurred in the direct-detection system after the fiber preamplifier, though the optically filtered power is now coupled into the fiber leading to the evanescent wave coupler, where 90% is coupled into the output fiber, thus adding an additional 10% optical loss not seen in the direct-detection case. The combined signal and LO powers are then coupled into the multimode fiber pig-

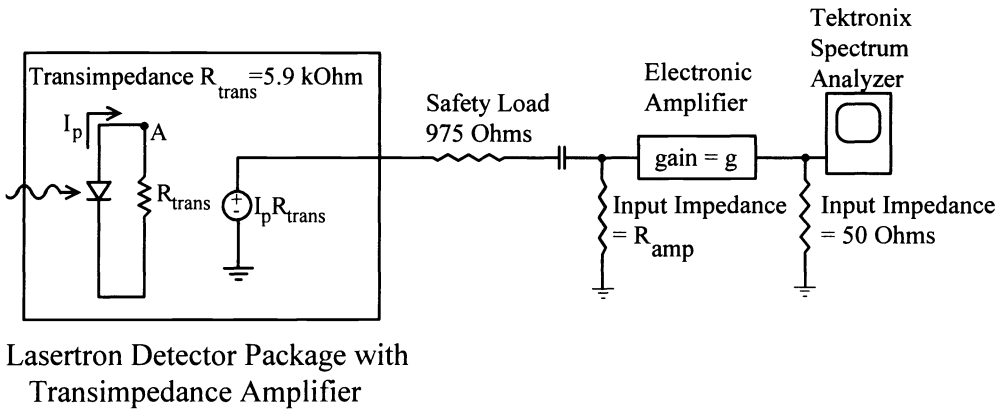

Fig. 4 Detection electronics. The detection electronics for both the direct and heterodyne detection ladar systems are shown here schematically. The Lasertron detector package includes both a photodetector and a current-to-voltage amplifier, and a safety load of 975 Ω is required to provide proper termination. An electronic amplifier is then used to boost the voltage level into the spectrum analyzer used to measure the SNR.

tailed to the detection electronics, where an intermediate frequency (IF) signal at 200 MHz is generated during the photodetection process. Again, the details of the detector and electronics are shown in Fig. 4, where for heterodyne detection g is the voltage gain of a Miteq electronic amplifier and R_{amp} is its input impedance. Note that the electronic amplifiers used for the two detection schemes differ in the frequency intervals of interest for each case (viz., 2 kHz for direct detection and 200 MHz for heterodyne detection).

With the system configurations thus established, the first issue we dealt with in our experimental plan was to determine the targets necessary to give measurable return signals for each detection scheme. Different types are required for both detection schemes because of the inherent differences in the detection techniques, though we mention that the theoretical and experimental results presented in the following sections are independent of the target type. All that is of interest is that we generate a small signal return. For instance, during direct detection, the return signal is not mixed with a large LO signal as it is in the heterodyne detection case. In order to generate a measurable return signal, we therefore decided to use a mirror-glint target for direct detection. This is acceptable if the transmitted, and thus the received, optical power is decreased, leaving the return signal power within the small-signal operating regime of the fiber amplifier. The variable-ratio attenuator (VRA), discussed previously (see Fig. 1), is used to accomplish this. By using the VRA, the strength of the return signal can be adjusted until it is just visible above the noise, with the fiber amplifier not in operation. When the amplifier is turned on then, the resulting ratio of signal to noise powers yields a direct measurement of the SNR improvement for the direct-detection case.

For the heterodyne-detection case, the large LO power mixes with the return signal power to create the IF signal, thus allowing a diffuse/speckle target to be used. The driver for the acousto-optic modulator, however, radiates an electric field at the desired 200-MHz IF signal frequency. This field tends to be picked up by the detection circuitry, resulting in a noise spike on the spectrum analyzer, which drowns out the IF signal at 200 MHz. To avoid this, the diffuse target was mounted on a motorized linear translation stage, thus causing a small Doppler shifting of the IF signal away from the 200-MHz noise spike. More specifically, the moving diffuse target consisted of a piece of flame-sprayed aluminum, tilted at 45 deg and translated at a constant velocity parallel to the beam path by a variable-speed micrometer.

To conclude this section, we have two final comments. First, in the preliminary preparations to take measurements verifying the results of these theoretical comparisons, it is

Table 1 List of variables. This table describes and quantifies the variables used in evaluating the SNR equations.[1] All variables common to both the direct and heterodyne detection equations are in the top section; the variables peculiar to either direct or heterodyne detection follow separately.

Common Variables

ν	- Optical power center frequency (1.064 μm)	= 2.82×10^{14} Hz
$\delta\nu$	- Spectrum analyzer resolution bandwidth	= 10 Hz
$\delta\nu_{opt}$	- Equivalent optical passband of the 4 nm filter	= 1.07×10^{12} Hz
η	- Detector quantum efficiency	= 0.82
h	- Planck's constant	= 6.626×10^{-34} J sec
G	- Fiber amplifier power gain	= 158
P_{se}	- Spontaneous emission power, G h ν $\delta\nu_{opt}$	= 31.3 μWatts
$P_{se,\delta\nu}$	- Incremental spontaneous emission power, G h ν δν	= 3.0×10^{-16} W
R_{trans}	- Integrated amplifier transimpedance	= 5900 Ω
R_{SA}	- Spectrum analyzer input impedance	= 50 Ω
$\Re$	- Detector responsivity (Lasertron Detector)	= 0.704 A/Watt
e	- Basic electronic charge	= 1.6×10^{-19} C
I_d	- Detector dark current (Lasertron Detector)	= 2.9 nA
k	- Boltzmann's constant	= 1.38×10^{-23} J/K
T	- Temperature	= 298 K

Direct Detection Variables

P_r	- Optical return signal power incident on the detector	= 0.4 nWatts
N	- Number of se-se beat components at 2 kHz	= 1.07×10^{11}
$\eta_{opt,d}$	- Optical efficiency between fiber amplifier and detector	= 0.56
g_a	- Analog Modules amplifier voltage gain	= 1000
R_a	- Analog Modules amplifier input impedance	= 1 MΩ

Heterodyne Detection Variables

P_r	- Optical return signal power incident on the detector	= 8×10^{-15} Watts
P_{lo}	- Local oscillator power, (near detector saturation power)	= 200 μWatts
$\eta_{opt,h}$	- Optical efficiency between fiber amplifier and detector	= 0.51
g_m	- Miteq amplifier voltage gain	= 1122
D	- Voltage divider effect (Heterodyne detection only)	= 0.048
R_m	- Miteq amplifier input impedance	= 50 Ω
N_h	- Number of se-se beat components at 200 MHz	= 1.05×10^{11}

important to realize that the neodymium dopant of the fiber has a four-level lasing scheme. Therefore, with the laser-diode pump light blocked, the return signal will pass through the fiber unamplified and with no loss due to signal absorption. This eliminates any need to physically remove the fiber amplifier from the system in order to make SNR measurement comparisons. Second, we again mention that in our previous analysis,[1,2] electrical SNR equations were developed with the goal of comparing the optical detection sensitivity of a ladar system with and without a fiber amplifier. In this paper, however, we directly examine the SNR equations and make SNR increase predictions for detection with the fiber amplifier included.

3 Prediction of Increases in Signal-to-Noise Ratio

The SNR equations we have previously derived[1,2] for the four test cases are used in this section to predict the SNR increases for ladar detection with a fiber amplifier included. The various noise terms are quantified numerically to give the predicted noise levels in decibels above 1 mW, while the values for all parameters used in the following analyses are given in Table 1.

3.1 *Direct-Detection SNR*

The SNR for direct detection without the fiber amplifier, $\mathrm{SNR}_{\mathrm{dir,wo}}$, expressed in terms of electrical power is given as[1]

$$\mathrm{SNR}_{\mathrm{dir,wo}}=\frac{\Gamma_{\mathrm{rl}}}{\Gamma_{\mathrm{SNl}}+\Gamma_{\mathrm{dark}}+\Gamma_{\mathrm{therm}}+\Gamma_{\mathrm{ea,A}}}, \tag{1}$$

where Γ_{rl} is the electrical signal power, Γ_{SNl} is the shot-noise power, Γ_{dark} is the dark-current noise power, Γ_{therm} is the thermal noise power, and $\Gamma_{\mathrm{ea,A}}$ is the electronic-amplifier noise power.

In practice, the signal power will appear on the spectrum analyzer as a narrowband signal centered at the frequency of the optical chopper, 2 kHz. The denominator of Eq. (1), however, is the total electrical noise power, shown on the spectrum-analyzer display as a noise level corresponding to the total noise divided into frequency components equivalent to the chosen frequency resolution. That is, for these experiments, the bandwidth intervals being examined are small, and the noise sources are considered white noises across these intervals. The noise power is therefore divided evenly across the spectrum-analyzer display. The noise level measured on the spectrum amplifier is then the amount of noise occurring in each frequency division, defined by the resolution bandwidth of the spectrum analyzer, $\delta\nu$, which we set to 10 Hz.

The terms in Eq. (1) are, of course, related to the various system parameters. For instance, based on our previous analysis, the electrical signal power is written as[1]

$$\Gamma_{\mathrm{rl}}=\frac{\frac{1}{2}(g_{\mathrm{a}}\Re P_{\mathrm{r}}R_{\mathrm{trans}})^2}{R_{\mathrm{SA}}}, \tag{2}$$

where g_a is the voltage gain of the Analog Modules electronic amplifier, $\Re$ is the responsivity of the detector, P_r is the optical return signal power incident *on the detector*, R_{trans} is the transimpedance of the detector package, and R_{SA} is the input impedance of the spectrum analyzer.

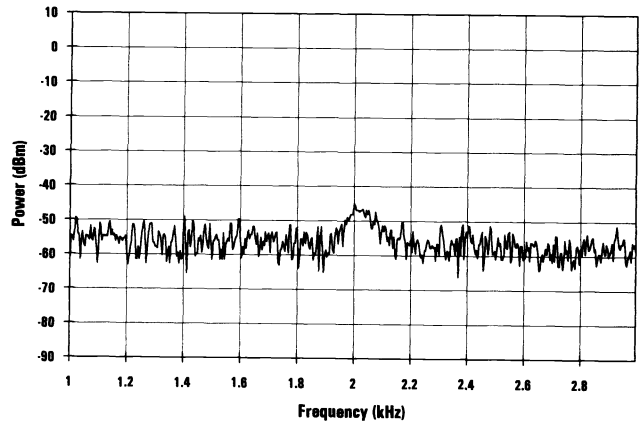

Fig. 5 Direct-detection signal without the fiber amplifier. This figure shows data taken from the spectrum analyzer for direct detection without the fiber amplifier. The direct-detection signal is located at 2 kHz. The noise level is −57.0 dBm and the signal level is −45.5 dBm, giving a SNR of 11.5 dB.

Because the optical-return signal powers were too small to be directly measured by available power meters, the power P_r incident on the detector was determined from Eq. (2) by setting the electrical signal power for direct detection without the fiber amplifier, Γ_{rl}, equal to its measured value of −45.5 dBm, or 28 nW. (See Fig. 5, which we will discuss in more detail later.) We then solve for P_r to obtain

$$P_{\mathrm{r}}=\frac{(2R_{\mathrm{SA}}\Gamma_{\mathrm{rl}})^{1/2}}{g_{\mathrm{a}}\Re R_{\mathrm{trans}}}=4\times10^{-10}\ \mathrm{W}\ . \tag{3}$$

Using this value for P_r, the following noise terms from Eq. (1) can now be evaluated[1]:

$$\Gamma_{\mathrm{SNl}}=\frac{(g_{\mathrm{a}}R_{\mathrm{trans}})^2[e(\delta\nu)\Re P_{\mathrm{r}}]}{R_{\mathrm{SA}}}=3.13\times10^{-16}\ \mathrm{W}\ , \tag{4}$$

$$\Gamma_{\mathrm{dark}}=\frac{(g_{\mathrm{a}}R_{\mathrm{trans}})^2\,[2e(\delta\nu)I_{\mathrm{d}}]}{R_{\mathrm{SA}}}=4.45\times10^{-15}\ \mathrm{W}\ , \tag{5}$$

$$\Gamma_{\mathrm{therm}}=\frac{(g_{\mathrm{a}}R_{\mathrm{trans}})^2[4k(\delta\nu)T/R_{\mathrm{trans}}]}{R_{\mathrm{SA}}}=1.9\times10^{-11}\ \mathrm{W}\ , \tag{6}$$

where e is the basic electronic charge, $\delta\nu$ is the resolution bandwidth of the spectrum analyzer, I_{d} is the detector dark current, k is the Boltzmann constant, and T is the temperature in kelvin. Note that Eq. (2) and Eqs. (4)–(6) are derived from the general electronic power equation,

$$\Gamma=\frac{\langle V^2\rangle}{R_{\mathrm{SA}}}\ . \tag{7}$$

where $\langle V^2\rangle$ is the mean squared signal voltage at the input of the spectrum analyzer.

Also note that the electronic amplifier noise power of Eq. (1) is a measured value. To perform this measurement, the

electronic amplifier input was disconnected from the detector package, and the output was measured on the spectrum analyzer, resulting in a measured amplifier noise value of

$$\Gamma_{ea,A} = 2.0 \times 10^{-9} \text{ W} . \quad (8)$$

As seen then from Eqs. (3)–(6), the measured electronic amplifier noise level of 2×10^{-9} W, or -57 dBm, is much larger than the other noise terms, thus allowing Eq. (1) to be simplified and evaluated as follows:

$$\text{SNR}_{\text{dir,wo}} = \frac{\Gamma_{r1}}{2 \times 10^{-9} \text{ W}} = 14.0 , \quad (9)$$

which corresponds to a SNR of 11.5 dB.

Similar to Eq. (1), the SNR for direct detection with the fiber amplifier, $\text{SNR}_{\text{dir,w}}$, is[1]

$$\text{SNR}_{\text{dir,w}} = \frac{\Gamma_{r2}}{\Gamma_{SN2} + \Gamma_{n,r\text{-}se} + \Gamma_{n,se\text{-}se} + \Gamma_{ea,A}} , \quad (10)$$

where Γ_{r2} is the amplified signal power, Γ_{SN2} is the shot-noise power, $\Gamma_{n,r\text{-}se}$ is the signal–spontaneous-emission beat noise power, $\Gamma_{n,se\text{-}se}$ is the spontaneous-emission–spontaneous-emission beat noise power, and $\Gamma_{ea,A}$ is the noise power of the Analog Modules electronic amplifier. Specifically, these terms are related to the system parameters as follows[1]:

$$\Gamma_{r2} = \frac{1/2(g_a \Re G P_r R_{trans})^2}{R_{SA}} = G^2 \Gamma_{r1} , \quad (11)$$

$$\Gamma_{SN2} = \frac{(g_a R_{trans})^2 \left\{ 2e(\delta\nu) \Re \left[G \cdot (P_r/2) + \eta_{opt,d} P_{se} \right] \right\}}{R_{SA}} , \quad (12)$$

$$\Gamma_{n,r\text{-}se} = \frac{(g_a R_{trans})^2 [\Re^2 G P_r (\eta_{opt,d} P_{se,\delta\nu})]}{R_{SA}} , \quad (13)$$

$$\Gamma_{n,se\text{-}se} = \frac{(g_a R_{trans})^2 (\Re \eta_{opt,d} P_{se,\delta\nu})^2}{R_{SA}} N , \quad (14)$$

$$\Gamma_{ea,A} = 2.0 \times 10^{-9} \text{ W} , \quad (15)$$

where the new quantities are the fiber-amplifier gain G, the total spontaneous-emission power P_{se}, the incremental spontaneous-emission power $P_{se,\delta\nu}$, the optical efficiency $\eta_{opt,d} = (0.75)(0.75) = 0.56$ of the direct detection system after the fiber preamplifier, and the number N of spontaneous-emission terms beating at the 2-kHz chopper frequency within the equivalent bandwidth of the 4-nm optical bandpass filter[1] (see Table 1).

Previously we determined[1] the fiber to yield a small-signal gain of about 1 dB/m. The fiber amplifier used for the work described herein was 22 m in length, giving approximately 22 dB of gain, or $G = 158$. Also, the spontaneous-emission power out of the fiber amplifier is dependent upon the gain as follows[6]:

$$P_{se} = Gh\nu S\nu_{opt} = 3.13 \times 10^{-5} \text{ W} , \quad (16)$$

where h is equal to Planck's constant, ν is the nominal spontaneous-emission frequency, and $S\nu_{opt}$ is the optical bandwidth. For this case, $\nu = 2.82 \times 10^{14}$ Hz is taken to be the bandpass-filter center frequency, corresponding to a wavelength of 1.064 μm, and $S\nu_{opt} = 1.07 \times 10^{12}$ Hz is the equivalent bandwidth of the 4-nm optical bandpass filter. With the optical signal power, spontaneous-emission power, and fiber-amplifier gain now known, the shot-noise power Γ_{SN2} is then calculated using Eq. (12) to be

$$\Gamma_{SN2} = 2.8 \times 10^{-11} \text{ W} . \quad (17)$$

For the terms expressing the return-signal–spontaneous-emission beat noise and the spontaneous-emission–spontaneous-emission beat noise, the spontaneous emission in an incremental bandwidth, $P_{se,\delta\nu}$, must be known. For convenience, the incremental bandwidth is chosen to be equal to the spectrum-analyzer resolution bandwidth $\delta\nu$, yielding

$$P_{se,\delta\nu} = \frac{P_{se}}{S\nu_{opt}} \delta\nu = 3.0 \times 10^{-16} \text{ W} . \quad (18)$$

$\Gamma_{n,r\text{-}se}$ is then determined to be

$$\Gamma_{n,r\text{-}se} = 3.6 \times 10^{-12} \text{ W} , \quad (19)$$

while the spontaneous-emission–spontaneous-emission beat-noise term, $\Gamma_{n,se\text{-}se}$, is found to be

$$\Gamma_{n,se\text{-}se} = 1.0 \times 10^{-9} \text{ W} , \quad (20)$$

thus giving a total noise level $\Gamma_{N,dir}$ for direct detection with the fiber amplifier of

$$\Gamma_{N,dir} = \Gamma_{SN2} + \Gamma_{n,r\text{-}se} + \Gamma_{n,se\text{-}se} + \Gamma_{ea,A} = 3.0 \times 10^{-9} \text{ W} . \quad (21)$$

This corresponds to a noise level of -55.0 dBm.

The predicted SNR for direct detection with the fiber amplifier is then found by substituting Eqs. (11) and (21) into Eq. (10), giving

$$\text{SNR}_{\text{dir,w}} = \frac{\Gamma_{r2}}{\Gamma_{SN2} + \Gamma_{n,r\text{-}se} + \Gamma_{n,se\text{-}se} + \Gamma_{ea,A}} = \frac{\Gamma_{r1} G^2}{\Gamma_{N,dir}} = 225806.5 , \quad (22)$$

which corresponds to a SNR of 53.5 dB. The predicted direct-detection increase in SNR, $\hat{\Delta}_d$, can then be obtained by subtracting (in dB) the SNR without the fiber amplifier from the predicted increase with the fiber amplifier, giving

$$\hat{\Delta}_d = 53.5 \text{ dB} - 11.5 \text{ dB} = 42.0 \text{ dB} . \quad (23)$$

3.2 *Heterodyne-Detection SNR*

We now examine heterodyne detection without the fiber amplifier. Ideally, the SNR for this case, $\text{SNR}_{\text{het,wo}}$, is given by[1]

$$\text{SNR}_{\text{het,wo}} = \frac{\Gamma_{IF1}}{\Gamma_{SN3}} , \quad (24)$$

where Γ_{IF1} is the IF electrical signal power and Γ_{SN3} is the LO shot-noise power, and it is assumed that the LO power has been increased until the LO shot-noise term dominates all other noises. Specifically in our previous analysis, we have shown that[1]

$$\Gamma_{IF1}=\frac{2(g_m D\Re R_{trans})^2}{R_{SA}}P_r P_{LO} \ , \tag{25}$$

$$\Gamma_{SN3}=\frac{(g_m D R_{trans})^2}{R_{SA}}2e\ \delta\nu\ \Re P_{LO} \ , \tag{26}$$

where g_m is the voltage gain of the Miteq electronic amplifier, D is the voltage-divider effect resulting from the 50-Ω input impedance of the Miteq amplifier and the 975-Ω series safety load required for the Lasertron detector package, and P_{LO} is the LO optical power (see Table 1). Note that the voltage-divider effect was not a factor in the direct-detection case, due to the large input impedance of the Analog Modules amplifier.

Physically, the IF signal is the term arising from the beating between the Doppler-shifted signal returning from the moving flame-sprayed aluminum target, discussed previously in Sec. 2, and the LO, which is frequently shifted by 200 MHz with respect to the outgoing beam of Fig. 3. Because of the target's motion, the IF signal will appear on the spectrum analyzer slightly shifted away from 200 MHz. In addition, the IF electrical signal power for heterodyne detection without the fiber amplifier, Γ_{IF1}, was measured (see Fig. 7, which will be discussed in more detail later) to be -55 dBm, or 3.2×10^{-9} W. This allows the optical power incident on the detector, P_r, to be calculated from Eq. (25):

$$P_r=\frac{R_{SA}\Gamma_{IF1}}{2P_{LO}(g_m D R_{trans}\Re)^2}=8.0\times10^{-15}\ \text{W} \ . \tag{27}$$

This value for P_r will be used later to evaluate the noise terms for heterodyne detection with the fiber amplifier.

Continuing our analysis for heterodyne detection without the fiber amplifier, however, LO shot-noise power, Γ_{SN3}, was calculated from Eq. (26) to be

$$\Gamma_{SN3}=9.1\times10^{-13}\ \text{W} \ , \tag{28}$$

corresponding to a noise level of -90.4 dBm. This value is approximately 10 dB larger than the electronic noise $\Gamma_{ea,M}$ from the Miteq amplifier, which was measured to be 6.4×10^{-14} W, or -101.9 dBm, thus verifying that our heterodyne detection system was nearly LO shot-noise limited. The predicted SNR for heterodyne detection without the fiber amplifier is therefore

$$SNR_{het,wo}=\frac{\Gamma_{IF1}}{\Gamma_{SN3}+\Gamma_{ea,M}}=\frac{3.2\times10^{-9}\ \text{W}}{9.74\times10^{-13}\ \text{W}}=3285.4 \ , \tag{29}$$

corresponding to a SNR of 35.2 dB, where we note that, for completeness, we have included both the shot-noise and the Miteq-amplifier-noise powers in the calculation of $SNR_{het,wo}$.

We now consider the case of heterodyne detection with the fiber amplifier, where the SNR equation, $SNR_{het,w}$, is given by[1,2]

$$SNR_{het,w}=\frac{\Gamma_{IF2}}{\Gamma_{SN4}+\Gamma_{n,r\text{-}se}+\Gamma_{n,LO\text{-}se}+\Gamma_{n,se\text{-}se}} \ . \tag{30}$$

where Γ_{IF2} is the amplified IF signal power, Γ_{SN4} is the shot-noise term when the fiber amplifier is included, $\Gamma_{n,r\text{-}se}$ is the return-signal–spontaneous-emission beat noise power, $\Gamma_{n,LO\text{-}se}$ is the LO–spontaneous-emission beat noise power, and $\Gamma_{n,se\text{-}se}$ is the spontaneous-emission–spontaneous-emission beat noise power term. Specifically, these terms are related to the system parameters as follows:[1,2]

$$\Gamma_{IF2}=\frac{2(g_m D\Re R_{trans})^2}{R_{SA}}GP_r P_{LO}=G\Gamma_{IF1} \ , \tag{31}$$

$$\Gamma_{SN4}=\frac{(g_m D R_{trans})^2}{R_{SA}}2e\ \delta\nu\ \Re(P_{LO}+\eta_{opt,h}P_{se}) \ , \tag{32}$$

$$\Gamma_{n,r\text{-}se}=\frac{(g_m D R_{trans})^2}{R_{SA}}2\Re^2 GP_r(\eta_{opt,h}P_{se,\delta\nu}) \tag{33}$$

$$\Gamma_{n,LO\text{-}se}=\frac{(g_m D R_{trans})^2}{R_{SA}}2\Re^2 P_{LO}(\eta_{opt,h}P_{se,\delta\nu}) \tag{34}$$

$$\Gamma_{n,se\text{-}se}=\frac{(g_m D R_{trans})^2}{R_{SA}}(\Re\eta_{opt,h}P_{se,\delta\nu})^2\ N_h \ , \tag{35}$$

where the new parameters are N_h, the number of spontaneous emission components beating together at the heterodyne frequency,[1] and the optical efficiency of the heterodyne system after the fiber amplifier, $\eta_{opt,h}=(0.75)(0.75)(0.9)=0.51$ (see Table 1).

Using Eq. (33) and the values of $P_{se,\delta\nu}$ and P_r given in Eqs. (18) and (27), respectively, the return-signal–spontaneous-emission noise is calculated to be

$$\Gamma_{n,r\text{-}se}=3.9\times10^{-19}\ \text{W} \ , \tag{36}$$

where we note that the spontaneous-emission power out of the fiber amplifier (P_{se}) and the fiber amplifier gain G are the same for both heterodyne detection and direct detection. Similarly, using Eq. (34) the LO–spontaneous-emission beat noise is found to be

$$\Gamma_{n,LO\text{-}se}=6.0\times10^{-11}\ \text{W} \ , \tag{37}$$

while the spontaneous-emission–spontaneous-emission beat noise from Eq. (35) is found to be

$$\Gamma_{n,se\text{-}se}=2.4\times10^{-12}\ \text{W} \ . \tag{38}$$

Also, using Eq. (32), the heterodyne-detection shot-noise term is calculated to be

$$\Gamma_{SN4}=9.2\times10^{-13}\ \text{W} \ , \tag{39}$$

thus giving a total noise level $\Gamma_{N,het}$ of

$$\Gamma_{N,het}=\Gamma_{SN4}+\Gamma_{n,r\text{-}se}+\Gamma_{n,LO\text{-}se}+\Gamma_{n,se\text{-}se}=6.4\times10^{-11}\ \text{W} \tag{40}$$

This corresponds to a noise level of -71.9 dBm.

The predicted SNR for heterodyne detection with the fiber amplifier is then found by substituting Eqs. (31) and (40) into Eq. (30), giving

$$\begin{aligned}\mathrm{SNR}_{\mathrm{het,w}} &= \frac{\Gamma_{\mathrm{IF2}}}{\Gamma_{\mathrm{SN4}}+\Gamma_{\mathrm{n,r\text{-}se}}+\Gamma_{\mathrm{n,LO\text{-}se}}+\Gamma_{\mathrm{n,se\text{-}se}}} \\ &= \frac{G\Gamma_{\mathrm{IF1}}}{\Gamma_{\mathrm{N,het}}} \\ &= 7900 \ , \end{aligned} \tag{41}$$

which corresponds to a SNR of 39.0 dB. The predicted SNR increase for heterodyne detection with the fiber amplifier, $\tilde{\Delta}_{\mathrm{h}}$, is then obtained by subtracting (in dB) the SNR for heterodyne detection without the fiber amplifier from the SNR for heterodyne detection with the fiber amplifier, giving

$$\begin{aligned}\tilde{\Delta}_{\mathrm{h}} &= 39.0 \text{ dB} - 35.2 \text{ dB} \\ &= 3.8 \text{ dB} \ . \end{aligned} \tag{42}$$

At this point it is important to examine this result carefully, as the classical result of using optical amplification in a heterodyne detection scheme is an increase in SNR by a factor approximately equal to the reciprocal of the quantum efficiency η (see Table 1) of the detector.[6] This chapter's analysis appears to contradict that result, before careful examination of the appropriate assumptions. In fact, in a heterodyne detection system, a fiber amplifier compensates for *any* losses after the fiber amplifier. The classical derivation assumes no losses between the optical amplifier and the detector, so the only sensitivity increase gained in adding a fiber amplifier is due to detector inefficiency. For the ladar testbed system we have used, however, there are additional optical losses after the fiber amplifier, collectively included in the heterodyne optical efficiency $\eta_{\mathrm{opt,h}}$. Including this efficiency factor (see Table 1), the expected sensitivity increase $\tilde{\Delta}_{\mathrm{hc}}$, according to classical theory,[6] is

$$\tilde{\Delta}_{\mathrm{hc}} = -10 \log\eta\eta_{\mathrm{opt,h}} = 3.8 \text{ dB} \ , \tag{43}$$

which is consistent with the result of our more rigorous analysis here. If the optical losses are absent, though, the resulting increase approaches the classical result. Therefore, even though very little increase in sensitivity can be achieved by the addition of a fiber amplifier to an *ideal* heterodyne detection scheme, for realistic systems the addition of a fiber amplifier is somewhat beneficial.

4 Experimental Data

In this section we present the SNR data we have taken and make comparisons between our measurements and the predicted values found in the previous sections. The first data taken were for direct detection without the fiber amplifier. Figure 5 shows the spectrum-analyzer display for this case, where we note that the average noise level is -57 dBm. Also note that this equals the measured value for the noise due to the electronic amplifier (Analog Modules amplifier) discussed in Sec. 3.1. This verifies our limiting-noise assumption for direct detection without the fiber amplifier. Also, the signal level in Fig. 5 is seen to be -45.5 dBm, which is equal to the value used in Eq. (3) to calculate the optical return signal power. The measured SNR is thus 11.5 dB.

With the inclusion of the fiber amplifier, the previous section predicts a direct-detection SNR increase of 42.0 dB. Figure 6 is a plot of the signal and noise for direct detection with the fiber amplifier turned on. The electrical signal power level is seen to be -1.1 dBm, while the noise level is -49.1 dBm, giving an experimental SNR of 48.0 dB. The experimental increase in SNR for direct detection with the fiber amplifier, Δ_{d}, is then obtained by subtracting (in dB) the SNR without the fiber amplifier from the SNR with the fiber amplifier:

$$\begin{aligned}\Delta_{\mathrm{d}} &= 48.0 \text{ dB} - 11.5 \text{ dB} \\ &= 36.5 \text{ dB} \ . \end{aligned} \tag{44}$$

This measured SNR increase is 5.5 dB smaller than the predicted increase of 42.0. In examining this discrepancy, we note that there are several errors inherent in the spectrum analyzer used. From the specifications given in the operator's manual, errors in the display dynamic range accuracy, RF attenuator range accuracy, and IF gain range accuracy are ± 2 dB, ± 1 dB and ± 2 dB, respectively, giving a possible cumulative error of ± 5 dB.

Next, Fig. 7 shows the Doppler-shifted IF signal for heterodyne detection without the fiber amplifier, located at 199.9982 MHz. The electrical signal power is seen to be -55 dBm, as was used to calculate the optical return signal in Eq. (26). The noise level is seen to be -91 dBm, which is equal to the calculated LO shot-noise power described in Sec. 3.2. These values give a SNR of 36 dB for heterodyne detection without the fiber amplifier.

Figure 8 is a plot of the signal and noise for heterodyne detection with the fiber amplifier turned on. The electrical signal power level is -33 dBm, while the noise level is -77 dBm, giving an experimental SNR of 44 dB. The experimental increase in SNR for heterodyne detection with the fiber amplifier, Δ_{h}, is obtained by subtracting (in dB) the SNR without the fiber amplifier from the SNR with the fiber amplifier:

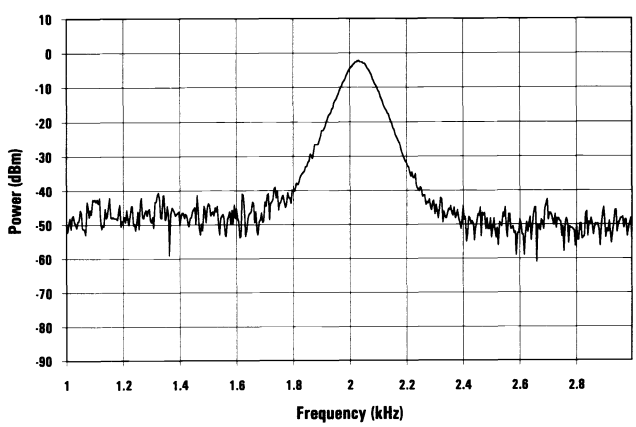

Fig. 6 Direct-detection signal with the fiber amplifier. This figure shows data taken from the spectrum analyzer for direct detection with the fiber amplifier. The direct detection signal is located at 2 kHz. The noise level is -49.1 dBm and the signal level is -1.1 dBm, giving a SNR of 48.0 dB.

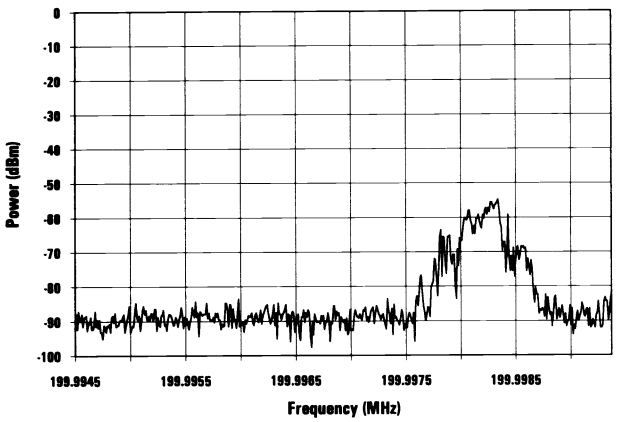

Fig. 7 Heterodyne-detection signal without the fiber amplifier. This figure shows data taken from the spectrum analyzer for heterodyne detection without the fiber amplifier. The heterodyne detection signal is located at 199.9982 MHz. As seen, this signal has a broad spectral width. This is due to jitter in the speed of the moving target, which results in corresponding variations in the Doppler shift. The noise level is -91 dBm and the signal level is -55.0 dBm, giving a SNR of 36 dB.

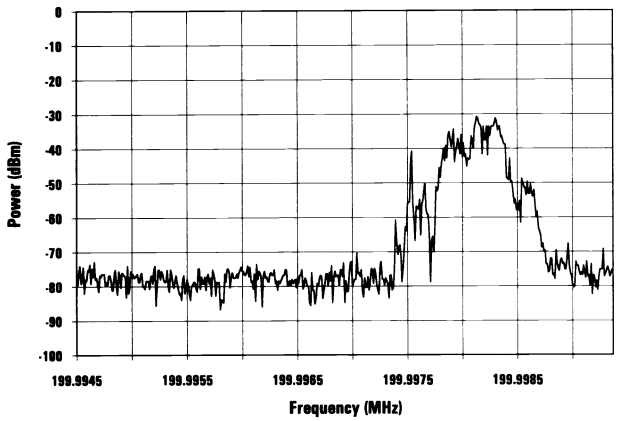

Fig. 8 Heterodyne-detection signal with the fiber amplifier. This figure shows data taken from the spectrum analyzer for heterodyne detection with the fiber amplifier. The heterodyne detection signal is located at 199.9982 MHz. The noise level is -77.0 dBm and the signal level is -33.0 dBm, giving a SNR of 44 dB.

$$\Delta_h = 44 \text{ dB} - 36 \text{ dB} = 8 \text{ dB} . \quad (45)$$

The measured increase in SNR is 4.2 dB larger than the predicted 3.8 dB, and the ± 5-dB uncertainty in the accuracy of the spectrum analyzer is again sufficient to account for the difference between the predicted and experimental SNR increases.

In comparing the direct and heterodyne detection results, it is somewhat disconcerting to see experimental results smaller than predicted for one case and larger than predicted in the other. This result is caused by the different power levels used by the two detection schemes. Specifically, the noise and amplified signal levels for the direct detection case are very near the maximum range of the spectrum analyzer, while the heterodyne-detection noise floors are near the minimum sensitivity level of the spectrum analyzer. These two extremes represent the difference between ± 5 dB in the accuracy, and it is reasonable to expect the experimental differences of the two cases to have opposite signs.

5 Summary

Previously we developed an electrical SNR model for direct and heterodyne detection with and without a fiber amplifier.[1,2] In this paper, experimental data have been presented and compared with theoretical predictions made using the equations developed in our previous work. For the direct-detection case, the measured SNR increase for detection with the fiber amplifier was 36.5 dB, which is 5.5 dB less than the predicted increase of 42.0 dB. For heterodyne detection, the measured SNR increase for detection with the fiber amplifier was 8.0 dB, which is 4.2 dB larger than the predicted increase of 3.8 dB. These values show a good match between theory and experiment, given the ± 5 dB uncertainty in the accuracy of the spectrum analyzer.

Further work with the ladar testbed is planned to examine fiber-amplifier performance in true ladar system functions such as ranging and target detection. This includes examining the effect of the fiber amplifier on return signals resulting from a pulsed or chirped output. There are also plans to expand the research into eyesafe wavelengths, such as erbium-doped fibers at 1.54 μm, which will allow us to take advantage of the advanced technology driven by the communication industry.

Acknowledgments

Helpful discussions with Edward Watson, Scott McCracken, Jay Overbeck, and Martin B. Mark of the Wright Laboratory Electro-Optic Techniques Group are gratefully acknowledged. Special thanks also to Mohammad A. Karim and the University of Dayton Research Council for their continuing support of the authors' research and scholarly activities. This work has been sponsored by the Wright Laboratory Avionics Directorate and Technology/Scientific Services, Inc., of Dayton, Ohio.

References

1. M. S. Salisbury, P. F. McManamon, and B. D. Duncan, "Sensitivity improvement of a 1-μm ladar system system incorporating an optical fiber preamplifier," *Opt. Eng.* **32**(11), 2671–2680 (Nov. 1993).
2. M. S. Salisbury, P. F. McManamon, and B. D. Duncan, "Erratum," *Opt. Eng.* **33**(12) (1994).
3. E. Snitzer, "Rare earth doped fiber lasers," in *Optical Fiber Communications '92 Conference Tutorial Sessions,* Tutorial FE, pp. 418–484 (Feb 4–7 1992).
4. R. E. Miers, "Fiber laser preamplifier for laser radar detectors," in *1991 USAF-RDL Summer Faculty Research Program Reports,* Vol. 5.B, Wright Laboratory Report 26, Wright Patterson Air Force Base, Ohio (July 1991).
5. A. V. Jelalian, *Laser Radar Systems,* p. 32, Table 1.1, Artech House, Boston (1992).
6. R. H. Kingston, *Detection of Optical and Infrared Radiation,* Chap. 8, Springer-Verlag, New York (1978).

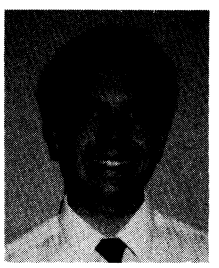

Michael S. Salisbury received BA degrees in physics and mathematics from North Central College in 1990. He obtained his MS degree in electro-optics from the University of Dayton while working as a research assistant at Wright Patterson Air Force Base in the Wright Laboratory Electro-Optic Sensors Group (WL/AARI-2). Since May of 1992, he has been employed by Technology Scientific Services Incorporated, Dayton, OH, as a

contractor assigned to the Wright Laboratory Electro-Optic Sensors facility. His research interests include optical-fiber amplifiers, solid-state ladar systems, ladar imaging, and remote sensing. Mr. Salisbury is a member of the Optical Society of America.

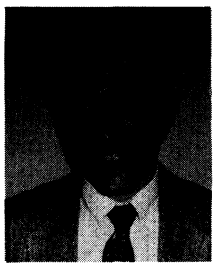

Paul F. McManamon received a BS degree in physics from John Carroll University. He then received the PhD degree from the Ohio State University in physics in 1977. Dr. McManamon has worked at Wright Patterson Air Force Base since 1968. His initial work was in the area of designing countermeasure waveforms against microwave radars. He then moved into electro-optical countermeasures and in 1979 took over the Thermal Imaging Group in the Air Force Avonics Laboratory, a position he held for eight years. More recently he has been performing technical work in laser radar and passive electro-optical sensors. He is currently acting chief of the Electro-Optics Branch, Mission Avionics Division, Avionics Directorate of Wright Laboratory.

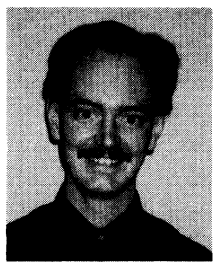

Bradley D. Duncan received the PhD degree in electrical engineering from Virginia Polytechnic Institute and State University (Virginia Tech) in 1991, after which he joined the University of Dayton faculty, where he has since held the position of assistant professor of electrical engineering and electro-optics. His research interests and activities span a wide range of areas within the optical sciences, including the study of fiber-optic sensor and system technology, integrated optics, acousto-optics, ladar imaging and system analysis, holography, and linear and nonlinear optical image processing. Dr. Duncan is a member of SPIE, the Optical Society of America, IEEE/Leos, and the American Society of Engineering Educators (ASEE).